Journal of The Electrochemical Society, **146** (5) 1966-1970 (1999)
S0013-4651(98)05-047-2 CCC: $7.00 © The Electrochemical Society, Inc.

Hydrogen Incorporation and Crystallization of Nanocrystalline Silicon Deposited by Electron Cyclotron Resonance Plasmas

S. Holgado,[z] J. Martínez, J. Garrido, and J. Piqueras

Laboratorio de Microelectrónica, Departamento de Ingeniería Informática and Departamento de Física Aplicada, Universidad Autónoma de Madrid, 28049 Madrid, Spain

Nanocrystalline silicon layers have been deposited by electron cyclotron resonance chemical vapor deposition from silane as precursor. Although hydrogen was not deliberately introduced in the plasma it was incorporated in the grown layers as evidenced by the presence of a main infrared absorption band around 2100 cm^{-1} with a shoulder at 2000 cm^{-1}. This suggests that most of the hydrogen is bonded to internal surfaces of microcavities instead of isolated Si–H bonds. In the first few hundreds, ~500 Å, of deposited layers, the estimated hydrogen concentration is rather low, below 5 atom %, and increases strongly for larger thicknesses. Solid phase crystallization at ~1100°C occurs in thin layers close to the substrates in which the hydrogen concentration is below a certain critical value of ~5 atom %.
© 1999 The Electrochemical Society. S0013-4651(98)05-047-2. All rights reserved.

Manuscript submitted May 18, 1998; revised manuscript received March 17, 1999.

Microcrystalline or nanocrystalline silicon (μc-Si or nc-Si) layers deposited at low temperatures are interesting as applications for solar cells, thin film transistors, and contacts to ultralarge scale integrated (ULSI) devices. During the last decade, there has been a large research effort in plasma enhanced chemical vapor deposition (PECVD) of silicon at low temperatures.[1-7] Special attention has been paid to the role played by the hydrogen present in the plasma and the way in which it is incorporated into the growing layer because (*i*) hydrogen tends to passivate dangling bonds enhancing the electrical activation of usual dopants,[8] and (*ii*) when a large amount of H is present in the plasma, μc-Si:H or nc-Si:H formation is favored instead of a-Si:H.[9-10]

Different mechanisms have been proposed to explain this trend: preferential etching of a-Si:H during deposition,[9] enhanced surface diffusion of the SiH_x adradicals induced by the large H flux, or some subsurface transformation of a-Si:H into μc-Si:H chemical annealing.[11] The control of such processes and the H bonding form in nc-Si:H may be of key importance for improving the performances of the deposited layers. Furthermore, because H outdiffuses easily at very low temperatures, a solid phase crystallization (SPC) process, similar to solid phase epitaxy (SPE) of amorphized ion implanted layers,[12] might take place at high temperatures. However, apart from the isolated Si–H bonds identified across an infrared (IR) absorption band at ~2000 cm^{-1}, [13,14] hydrogen is arranged in different configurations into the growing layer depending on the method and deposition conditions.

Hydrogen bonded to internal surfaces[15] or $(SiH_2)_n$ chains[16] in cavities or voids is believed to be the origin of the 2100 cm^{-1} absorption band observed in a-Si:H structure. Hydrogen ion implantations to [H] > 3 atom % also gives rise to the 2100 cm^{-1} band attributed to Si–H clustering.[17] High density H-plasma exposure, radio frequency (rf) or electron cyclotron resonance (ECR), of amorphized ion implanted Si leads also to the appearance of an additional band at 2080 cm^{-1} when [H] > 6 atom % and solid phase epitaxy does not occur when this threshold value is exceeded.[18]

Apparently, the presence of H in the plasma, because it is deliberately introduced or because it is released from the fragmented Si precursors, eg., silane, might lead to structural modifications and internal microcavities or voids preventing solid phase crystallization. Furthermore, etching by the H plasma and Si redeposition processes, termed "surface models,"[18,19] might give rise to nanocrystallites deposition, random nucleation, and growth. This is evidenced across the morphology of silicon surfaces etched in a H plasma. In Si(111), the surface roughness induced by the plasma etch is rather low, and in Si(100), a large roughness is produced. Later growth by ECR plasma CVD enhances the roughness preventing solid phase crystallization of nc-Si layers deposited on Si(100). [20]

In this paper, we report H incorporation in nc-Si layers deposited by ECR plasma CVD without intentional H introduction. Crystallization and hydrogen loss during annealing at high temperatures were investigated by means of spectroscopic ellipsometry (SE) and Fourier transform infrared spectroscopy (FTIR).

Experimental

The ECR plasma was formed by introducing 100 standard cubic centimeters per minute (sccm) of Ar directly into the resonance zone, whereas the reactive gas, 40 sccm of 5% SiH_4 (diluted in Ar), was introduced out of the resonance zone via a second gas inlet close to the substrate holder. The pressure in the reaction chamber under these conditions was 2 mTorr. A microwave power of 100 W was used in all the cases and the samples were not intentionally heated. In a separate experiment, under similar conditions, we observed that the plasma made the temperature rise to nearly 300°C in a few minutes.

nc-Si layers were deposited on p-type (resistivity 4-6 Ω cm) Czochralski Si wafers by plasma ECR-CVD. The substrates were etched in 30% HF diluted in ethanol and then rinsed in pure ethanol prior to loading into the vacuum chamber. This cleaning procedure removes the native oxide and passivates the silicon surface to delay its oxidation. Because we have previously found significant differences between the morphology and optical properties of the layers deposited on (100) and (111) oriented Si wafers,[20] both orientations were used in these experiments. However, in this work, neither sample was in situ cleaned by Ar + H_2 plasma, and H_2 was not deliberately introduced during deposition.

Samples with different thicknesses were deposited for 30, 60, 120, 240, and 480 s, hereafter referred as samples 1 to 5, respectively.

After deposition, the wafers were cut into small pieces and then subjected to isochronal thermal treatments at different temperatures, 700, 800, 900, 1000, and 1100°C, in a rapid thermal annealing (RTA) furnace under a nitrogen ambient. The temperature rise time was about 5 s.

Spectroscopic ellipsometry is a characterization technique that is very sensitive to the crystalline state of surface layers with a good in-depth accuracy. The ellipsometric angles Ψ y Δ of the different samples were measured by means of a phase modulated SE UVISEL from Jobin Ivon between 1.5 and 4.5 eV. From Ψ y Δ, an effective dielectric constant, usually termed pseudoelectric constant, of the overall sample, layer plus substrate, can be obtained. This pseudoelectric constant was simulated by an air/native oxide/layer/c-Si substrate structure using the Bruggeman effective medium approximation (EMA). μc-or nc-Si has a dielectric constant which differs considerably from that of amorphous or crystalline silicon and depends

[z] E-mail: Susana.Holgado@ii.uam.es

Downloaded on 2014-12-01 to IP 150.244.139.47 address. Redistribution subject to ECS terms of use (see ecsdl.org/site/terms_use) unless CC License in place (see abstract).

S0013-4651(98)05-047-2 CCC: $7.00 © The Electrochemical Society, Inc.

strongly on the structure conditions, and method of deposition. However, the disordered regions between grains can be simulated by including some a-Si percentage and the lack of compacity by void addition.[21,27] Thus a mixture of a-Si, c-Si, and voids was used to get an idea of the crystallinity degree of the nc-Si layers. Both thickness and composition were considered as parameters to fit the experimental results. In the case of the unannealed samples, two layers with different composition were required to get a good fit of the experimental results.

To investigate the chemical bonding and hydrogen concentration in the layers, Fourier transform infrared measurements in transmission mode were performed with a Bruker IFS 66V spectrometer. For these measurements, the layers were deposited on high resistivity float zone (FZ) Si(100) wafers. The oxygen content in the substrate, as tested also by infrared spectroscopy, was below 0.5 ppma.

Results

Ellipsometry.—Contrary to what happens when the substrates were in situ cleaned with Ar + H_2 plasma and intentional H_2 added to the plasma,[20] here, we do not find significant differences between the pseudodielectric constant of the samples deposited on (100) and (111) Si wafers. Samples 1 and 4 deposited on (100) substrates were chosen to follow the behavior of the dielectric constant with the annealings. The first was chosen because it has the thinnest nc-Si layer and the second was chosen because it was deposited for one of the largest times. Figure 1 shows the dielectric constant of both samples, as-deposited and after 800 and 1100°C heat-treatments for 30 s. Note that as the annealing temperature increases, the critical points (CP) at ~3.4 and 4.2 eV of the imaginary part of the dielectric constant became apparent, resembling that of c-Si. Moreover, the SE spectrum of sample 1 after a 1100°C annealing is very similar to that of c-Si, whereas, in the SE spectrum of sample 4, the second maximum at 4.2 eV is not well defined.

As noted earlier, in the case of as-deposited samples, the assumption of an nc-Si single layer did not give an accurate account of the experimental results, and, precise simulations require two layers with different compositions. The best fit for sample 1 was a first layer, close to the Si substrate, (layer 1) of 322 Å with a 42% a-Si, 43% c-Si, and 15% of voids, and an outer layer (layer 2) of 134 Å with 74% of a-Si, 26% of voids, and no c-Si. In sample 4, layer 1 has a thickness of 330 Å and a composition of 43% a-Si, 52% c-Si, and 5% voids whereas layer 2 has 776 Å with a composition of 68% a-Si, 1% c-Si, and 31% voids. After the first heat-treatment at 700°C (SE spectrum not shown in Fig. 1) only one layer of 642 Å thickness and 77% of a-Si, 5% of c-Si, and 18% of voids, not too much different from layer 2 of the unannealed sample 4, was required. This can be qualitatively viewed as the SPC of a rather ordered layer close to the substrate (more or less coincident with layer 1) and a slight thickness reduction and disorder increase of the outer layer. Increasing temperature annealings did not change too much the thickness but the crystalline fraction increases at the expense of the a-Si and voids contents.

In sample 1, layer 1 seems also to disappear and the thickness of layer 2 decreases but the crystalline fraction of layer 2 increases even with the first heat treatment at 700°C. After the 1100°C annealing, the SE spectrum of sample 1 is undistinguishable from that of c-Si, indicating complete crystallization of the deposited layer.

Note that layer 1 is very similar in all the as-deposited samples with a thickness ranging from 322 to 339 Å and composition 42-44% a-Si, 43-51% of c-Si, and 5-15% of voids. In contrast, layer 2 has a small or even negligible c-Si content in all of the samples. Furthermore, the behavior of layer 2 with annealings differs from sample 1 to the rest. Whereas, the a-Si fraction in sample 1 seems to decrease even from the first anneal, in the other samples initially, at 700°C, it increases, and later decreases continuously. However, the most important difference is that at 1100°C, layer 2 has completely disap-

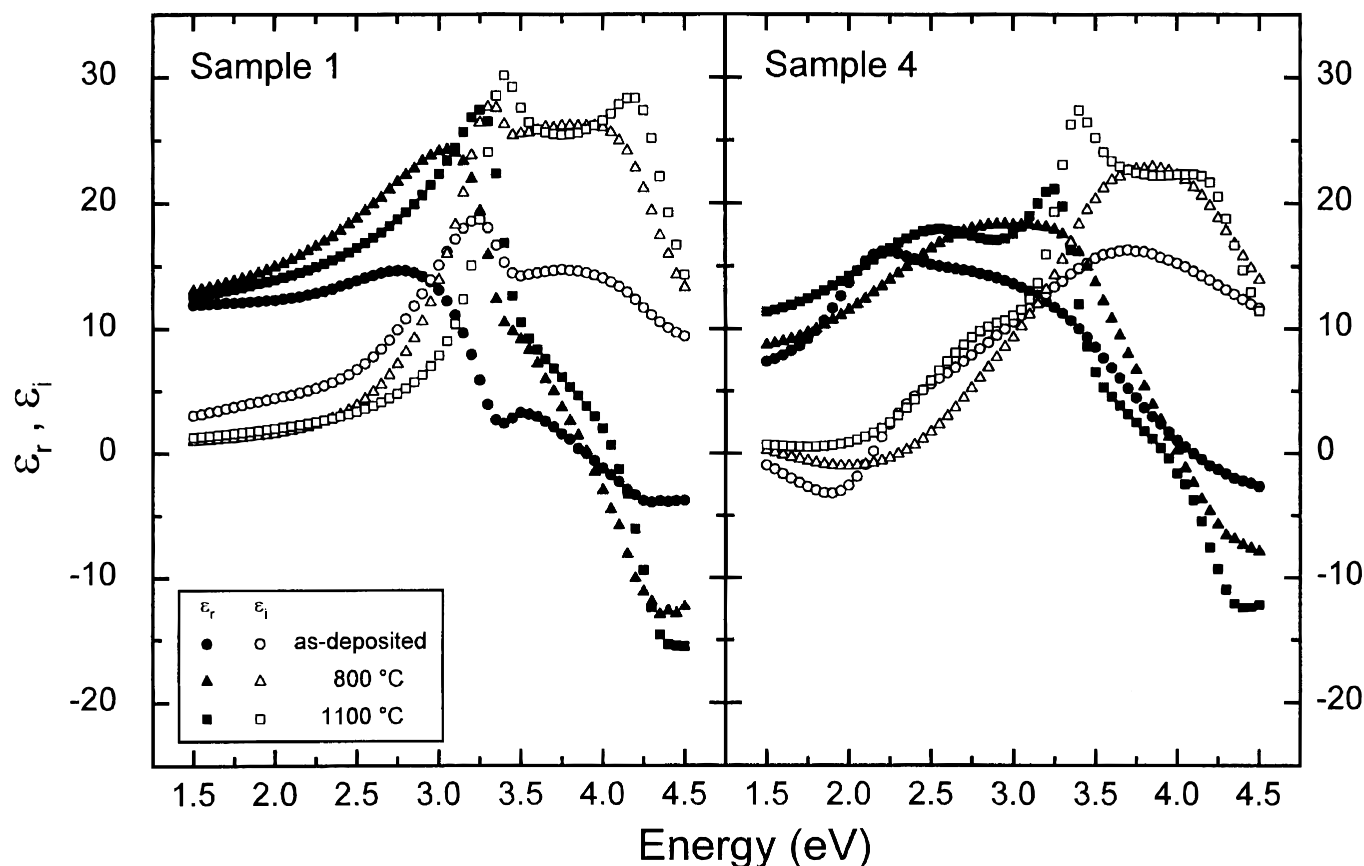

Figure 1. Real, ϵ_r, and imaginary, ϵ_i, parts of the pseudodielectric constant of samples 1 and 4, as deposited, and after 800 and 1100°C annealings.

Downloaded on 2014-12-01 to IP 150.244.139.47 address. Redistribution subject to ECS terms of use (see ecsdl.org/site/terms_use) unless CC License in place (see abstract).

S0013-4651(98)05-047-2 CCC: $7.00 © The Electrochemical Society, Inc.

peared in sample 1 whereas in the remaining samples the thickness of layer 2 is reduced to about half of that of the unannealed sample with the first anneal (700°C), and later heat-treatments did not change appreciably the thickness. The a-Si and c-Si fractions of layer 2 are shown in Fig. 2a and b, respectively, the rest (not shown) being voids percent. As can be seen (Fig. 2a) and c-Si fraction of layer 2 increases with the annealing temperature reaching values between 66 to 91% in samples 2 to 4. Consequently, the a-Si content decreases with the temperature up to final values between 3 to 23%. It should be mentioned that the final a-Si fraction, after the highest annealing temperature, is the largest one for the thickest deposited layer. In sample 5, the deposited layer was considerably degraded, probably because of mechanical stresses generated by the large content of voids after the 1000°C anneal, and thus, possible fits lack significance.

Infrared transmissions.—Infrared transmissions have been converted into absorbances using the layer thicknesses of the best fits to the experimental SE spectra. Figure 3 shows the absorption constants of samples 4 and 5, as-deposited (0°C), and after several annealings. Hydrogen incorporation into the nc-Si layers is evidenced from the appearance of a 2100 cm^{-1} band with a shoulder at 2000 cm^{-1}, in contrast with the observation in the electrochemically prepared "porous silicon" region, in which three bands due to SiH_x, $x = 1$ to 3, appear. The last one is associated to the Si–H stretching vibration, whereas the 2100 cm^{-1} has been attributed to hydrogen bonded to internal surfaces of cavities or voids within an a-Si:H[15] or a nc-Si:H structure.[18] Further, a band at around 1000 cm^{-1} has been observed in all the samples. This band is in the region of Si–O–Si asymmetric vibration in substoichiometric SiO_x.

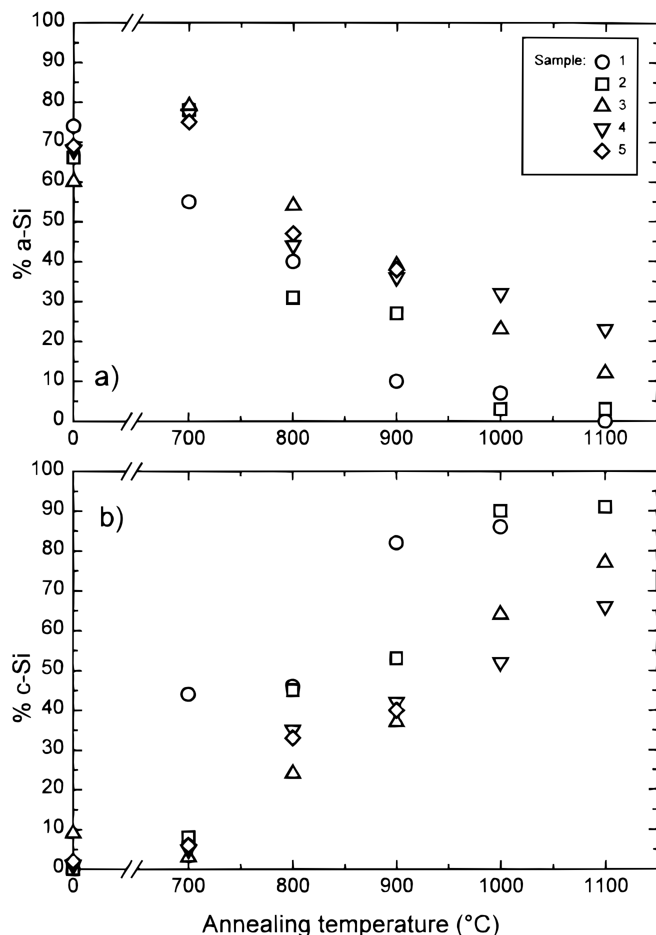

Figure 2. (a) a-Si and (b) c-Si fractions of layer 2 after the annealing temperature.

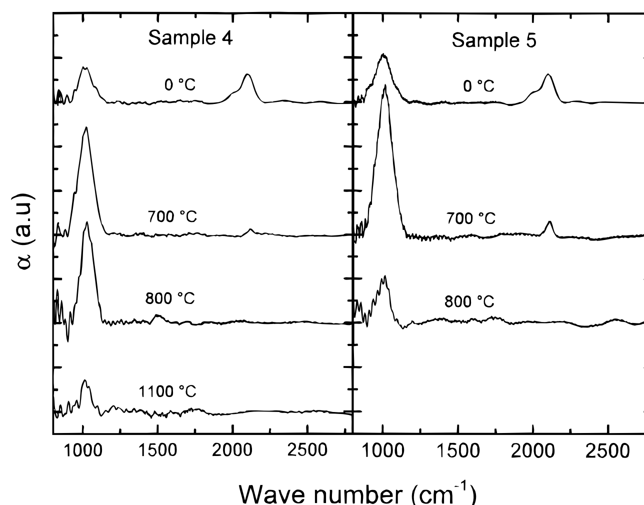

Figure 3. IR absorption coefficients of samples 4 and 5, as-deposited, and after 700, 800, and 1100°C annealings.

Pai et al.[23] found that the Si–O stretching frequency shifts from 940 cm^{-1} in oxygen doped Si to 1075 cm^{-1} in stoichiometric SiO_2. If this were the origin of the 1000 cm^{-1} band, this should correspond to SiO_x inclusions with $x = 1$. [23] Deliberate introduction of H_2 during the film growth did not prevent the 1000 cm^{-1} band appearance even when the H_2 was purified across an Ag-Pd membrane.

Both Si-H related bands decrease with the annealing temperature being negligible after the 800°C treatment in all the samples. Figure 4 illustrates the annealing temperature behavior of the integrated area of the three bands. Only a band area comparison has been done because of the uncertainty of the 1000 cm^{-1} band assignment and thus of its absorptivity. As can be seen, the 1000 cm^{-1} band area increases after the 700°C annealing, apparently at the expense of the 2000 and 2100 cm^{-1} bands. For temperatures over 700°C, the 1000 cm^{-1} band area also decreases continuously, suggesting that the defects originating this band are being annihilated or becoming optically inactive.

Figure 5 shows the 2000 cm^{-1} region of the IR spectra of the as-deposited samples. The IR spectra are deconvoluted into two Gaussians except in the case of sample 1 in which the 2000 cm^{-1} contribution is undistinguishable from noise. Using the calibration factors, $A_{2000} = 7.4 \times 10^{19}$ cm^{-2} and $A_{2100} = 2.1 \times 10^{20}$ cm^{-2} previously reported in the literature[16,24] the H concentration in the five samples have been calculated. Table I summarizes the exact peak positions, the integrated band areas ,and the hydrogen concentration associated

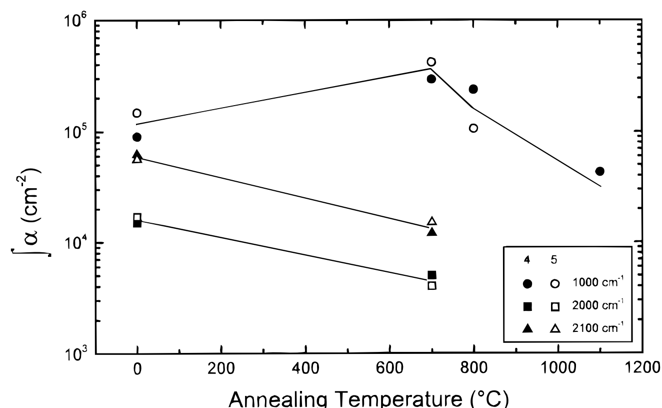

Figure 4. 1000, 2000, and 2100 cm^{-1} integrated band areas of samples 4 and 5, as-deposited, and after 700, 800, and 1100°C annealings. Continuous lines are added as a visual aid.

Downloaded on 2014-12-01 to IP 150.244.139.47 address. Redistribution subject to ECS terms of use (see ecsdl.org/site/terms_use) unless CC License in place (see abstract).

S0013-4651(98)05-047-2 CCC: $7.00 © The Electrochemical Society, Inc.

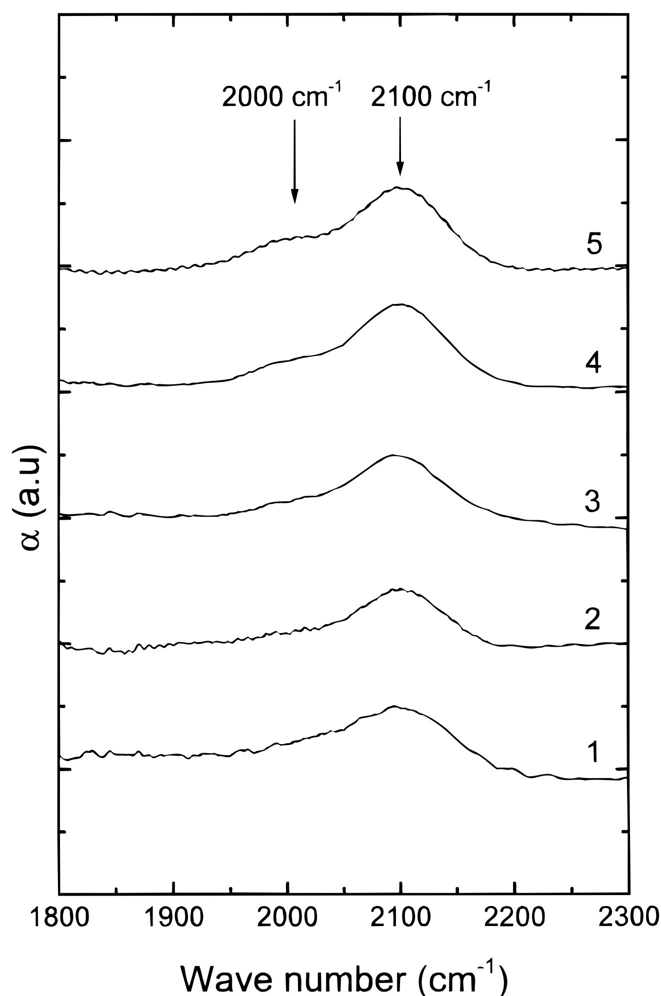

Figure 5. Absorption coefficients of Si–H, 2000 and 2100 cm^{-1}, associated bands of the as-deposited samples.

with each of the two bands. As can be seen, the H concentration in any of the two positions increases with the layer thickness supporting the above assumption of two nc-Si layers of different composition to simulate the experimental pseudodielectric constant. A qualitative idea of the H incorporation with the increasing thickness can be obtained by subtracting the integrated band area of a given sample from the following in increasing order and dividing this difference by the incremental thickness. Figure 6 illustrates the result of such an operation. A dotted line corresponding to [H] ≅ 5 atom % has been added to the plot. This concentration is about the same, 3%, for which large dose H^+ implantations in a-Si give rise to structural modifications and the appearance of the 2100 cm^{-1} band attributed to Si–H clustering.[17] In a previous paper, we reported that plasma hydrogenation of ion implanted Si to H concentrations exceeding ~6% gives rise to the formation of voids in a near subsurface region and the appearance of the 2100 cm^{-1} band.[18] Over this [H], the a-Si structure is modified and solid phase crystallization does not occur. As can be seen in Fig. 6, only sample 1 has a total [H] below this threshold value, 5%, justifying why this sample was the only one that completely crystallized. Apparently, the H incorporation to the growing layer suddenly increases after the first ~500 Å of the grown layer. For thicknesses over this value, the [H] seems to decrease slowly.

Discussion

Although the 1000 cm^{-1} is in the SiO_x region,[23] its origin could be complex because its area increases while the two Si–H bands decrease. Further, after the 700°C annealing, once the two Si–H bands have became negligible, the 1000 cm^{-1} band also decreases. If these complex centers are hydrogen related, additional H losses from them might explain the decrease after 700°C.

Table I. Peak positions, integrated absorption coefficients, and bond densities of the Si–H stretching modes.

	Stretching modes of Si–H		
Sample	Peak position (cm^{-1})	$\int\alpha \times 10^4$ (cm^{-2})	$N \times 10^{21}$ (cm^{-3})
1	2095	0.2	0.22
2	2023	1.0	0.37
	2103	3.4	3.42
3	2005	1.1	0.46
	2099	4.6	4.60
4	2003	1.5	0.56
	2101	6.2	6.15
5	2005	1.8	0.65
	2100	6.6	6.60

Infrared measurements show that the 2100 cm^{-1} band dominates over the 2000 cm^{-1} one even in the regions close to the substrate or very thin layers, with [H] < 5 atom %, indicating that most of the H is bonded to internal surfaces of microcavities. In fact, ECR-CVD generates large amounts of ions and H activated species, and thus, the H incorporation is expected to occur similarly to that in plasma hydrogenation of amorphous ion implanted layers.[18] After the first few hundreds of angstroms, ~500 Å, H bond densities associated to both 2000 and 2100 cm^{-1} bands increase strongly. However, isolated Si–H bond densities remain below the critical concentration.

Because mean [H] values have been obtained by subtracting the H content of the different layer deposited under the same conditions, and dividing by the thickness difference, Fig. 6 cannot be taken as a true profile and the actual [H] values may differ from that shown. However, the trend of H buildup after the first ~500 Å of growing layer is clear. According to the "surface models" of μc-si growth,[10,19] a surface phase, below which the a-Si:H to μc-Si:H transformation occurs, should be formed. However, as in this case, H is not intentionally introduced, the buildup of H in the surface layer may be delayed for a time, after which [H] overcomes the critical value, ~5 atom %.

SE measurements show that only sample 1 which has a thickness of ~500 Å has completely crystallized at 1100°C. In the other samples only layer 1 of ~330 Å, close to the substrate, has crystallized although the transformation to c-Si of a part of layer 2 cannot be discarded.

The presence of H bonded to internal surfaces of microcavities seems to be associated with the inhibition of the crystallization

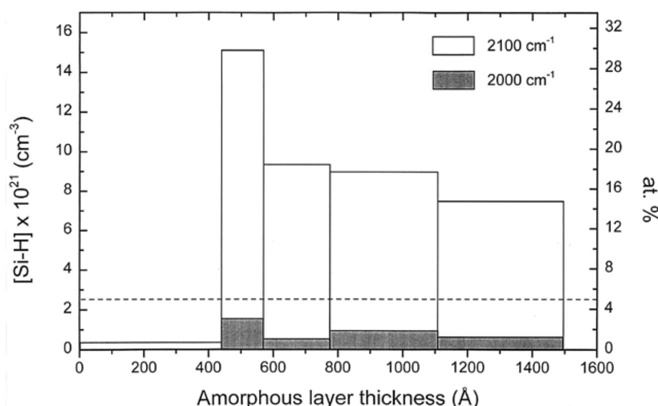

Figure 6. Mean H concentration as a function of the incremental thickness of the layer estimated from the 2000 and 2100 cm^{-1} band areas. The dotted line indicates 5 atom %.

Downloaded on 2014-12-01 to IP 150.244.139.47 address. Redistribution subject to ECS terms of use (see ecsdl.org/site/terms_use) unless CC License in place (see abstract).

S0013-4651(98)05-047-2 CCC: $7.00 © The Electrochemical Society, Inc.

process of nc-Si. However, because the layers close to the substrate have completely crystallized with the annealings, the no crystallization must more likely caused by an excessive H concentration. When [H] exceed about 5 atom % large voids are generated giving rise to high crystallite disorientation and stresses that cannot be recovered with the annealings.

Conclusions

Hydrogen is incorporated into nc-Si layers deposited by ECR-CVD even when it is not deliberately introduced. The H incorporation is mainly evidenced from presence of the 2100 cm^{-1} band associated to H bonded to internal surfaces of microcavities, whereas, the 2000 cm^{-1} band, usually associated to isolate Si–H bonds, appears only as a shoulder of the former one. The first few hundreds of angstroms of the grown layers are relatively free from H, and solid phase crystallization occurs at ~1100°C. Beyond the first ~500 Å, larger amounts of H are incorporated to the growing layer. Although after the highest temperature annealings hydrogen seems to be reduced to negligible concentrations, the microcavities associated to the initial H clusters could remain after the heat-treatments preventing complete solid phase crystallization.

S. Holgado assisted in meeting the publication costs of this article.

References

1. K. Fukuda, J. Murota, S. Ono, T. Matsuura, H. Uetake, and T. Ohmi, *Appl. Phys. Lett*., **59**, 2853 (1991).
2. K. Yokota, T. Sugahara, K. Kinoshita, S. Tamura, and S. Katayama, *J. Electrochem. Soc*., **140**, 525 (1993).
3. H. Shirai, *Jpn. J. Appl. Phys*., **34**, 450 (1995).
4. C. Godet, N. Layadi, and P. Roca i Cabarrocas, *Appl. Phys. Lett*., **66**, 3146 (1995).
5. T. Akasaka and I. Shimizu, *Appl. Phys. Lett*., **66**, 3441 (1995).
6. P. Roca i Cabarrocas, N. layadi, T. Heitz, E. Adams, B. Drévillon, and I. Solomon, *Appl. Phys. Lett*., **66**, 3609 (1995).
7. W. J. Varhue, P. S. Andry, J. L. Rogers, E. Adams, R. Kontra, and M. Lavoie, *Solid State Technol*., **39**, 163 (1996).
8. W. E. Spear and P. E. LeComber, *Solid State Commun*., **17**, 1193 (1975).
9. S. Veprek, M. Heintze, F. A. Sarot, M. Jurzik-Rajman, and P. Willmodt, *Mater. Res. Soc. Symp. Proc*., **118**, 3 (1988).
10. C. C. Tsai, G. B. Anderson, R. Thompson, and B. Wacker, *J. Non-Cryst. Solids*, **114**, 151 (1989).
11. N. Shibata, K. Fukuda, H. Ohtoshi, J. Hanna, S. Oda, and I. Shimizu, *Mater. Res. Soc. Symp. Proc*., **95**, 225 (1987).
12. J. M. Poate, K. N. Tu, and J. W. Mayer, *Thin Films: Interdiffusion and Reactions*, Chap. 12, Wiley & Sons Inc., New York (1978).
13. M. H. Brodsky, M. Cardona, and J. Cuomo, *Phys. Rev. B*, **16**, 3556 (1977).
14. H. Shanks, C. J. Fang, L. Ley, M. Cardona, F. J. Demond, and S. Kalbitzer, *Phys. Status Solidi B*, **100**, 43 (1980).
15. H. Wagner and W. Beyer, *Solid Sate Commun*., **48**, 585 (1983).
16. C. Manfredotti, F. Fizzotti, M. Boero, P. Pastorino, P. Polosello, and E. Vittone, *Phys. Rev. B*, **50** (1994).
17. S. Acco, D. L. Williamson, P. A. Stolk, F. W. Saris, M. J. van der Boogaard, W. C. Sinke, W. F. van der Berg, S. Roorda, and P. C. Zalm, *Phys. Rev. B*, **53**, 4415 (1996).
18. S. A. McQuaid, S. Holgado, J. Garrido, J. Martínez, J. Piqueras, R. C. Newman, and J. H. Tucker, *J. Appl. Phys*., **81**, 7612 (1997).
19. I. Solomon, B. Drévillon, H. Shirai, and N. Layadi, *J. Non-Cryst. Solids*, **164-166**, 989 (1993).
20. S. Holgado, J. Martínez, J. Garrido, C. Morant, and J. Piqueras, *Appl. Phys. Lett*., **69**, 1873 (1996).
21. B. G. Bagley, D. E. Aspnes, A. C. Adams, and C. J. Mogab, *Appl. Phys. Lett*., **38**, 56 (1981).
22. K. Vedam, P. J. McMarr, and J. Narayan, *Appl. Phys. Lett*., **47**, 339 (1985).
23. P. G. Pai, S. S. Chao, Y. Tagaki, and G. Lucovsky, *J. Vac. Sci. Technol., A*, **4**, 689 (1986).
24. A. A. Langford, M. L. Fleet, B. P. Nelson, W. A. Lanford, and N. Maley, *Phys. Rev. B*, **45**, 13367 (1992).

Downloaded on 2014-12-01 to IP 150.244.139.47 address. Redistribution subject to ECS terms of use (see ecsdl.org/site/terms_use) unless CC License in place (see abstract).